Electrical characterization of LiTaO$_3$:P(VDF–TrFE) composites

Padmaja Guggilla · A. K. Batra · M. E. Edwards

Abstract Composites of pyroelectric ceramics and polymers are very important as their unique features and properties can be easily tailored for various specific applications. Lithium tantalatum oxide (LiTaO$_3$, LT), the pyroelectric ceramic powder has been incorporated into a polyvinylidene fluoride–trifluoroethylene [P(VDF–TrFE) 70/30 mol%] copolymer matrix to form 0–3 composites. The composite films were prepared using 'solvent casting' (SC) method to disperse the ceramic powder homogeneously in the P(VDF–TrFE) copolymer matrix with various wt% of LT powder. In order to derive high pyroelectric performance, the samples were poled. Electric properties, such as the dielectric constant, dielectric loss, and pyroelectric coefficient, have been measured as a function of temperature and frequency. In addition, material figures-of-merit, very important factors for assessing many sensor applications have also been calculated. The results show that the fabricated lead free lithium tantalite: P(VDF–TrFE) composite materials have a good potential for pyroelectric infrared sensor applications.

Introduction

Pyroelectric materials are of significant interest as they are very useful in the detection of the infrared (IR) radiation with the wavelengths ranging between 3–5 and 8–14 μm without the need of cooling [1]. Detection of such radiation used in many applications such as thermal imaging, fire detection, motion sensing, and robotics. When pyroelectrics are heated, the internal electric charges are scattered in such a fashion that positive and negative poles are formed [2]. This alignment is permanent unless the field is reversed or a mechanical disturbance, such as produced heat destroys the alignment. Currently, lithium tantalite (LiTaO$_3$), triglycine sulfate (TGS) single crystals, and certain ceramics (PZT) are most widely used, because of their characteristic ferroelectric, piezoelectric, and pyroelectric properties. These materials require high temperatures, and must be cut, lapped and polished down to the required thickness which is an expensive and cumbersome process [3]. Constant demands for new material system for specific applications dictate the scientists to focus on thin films rather than bulk ceramics or single crystals, especially composite films [4]. Thin and thick film technologies offer many advantages over bulk ceramics. In recent years, there is a great need for composites because the combination of two or more materials can lead to performance enhancement [5]. The composites consist of two or more chemically different materials or phases. In these materials, it is possible to tailor their electrical and mechanical properties catering a variety of applications' demand. Recent studies on ceramic–polymer based pyroelectric composites show potential usefulness via large area, lightweight, enhanced strength, and flexible IR sensing behavior [2]. The hybrid properties of composites comprise large pyroelectric coefficients of ceramic material and excellent mechanical strength, flexibility, formability, and robustness of the polymer. Thus, the properties of these composites depend on the following factors: (i) properties of its individual constituents (ingredients); (ii) volume fraction of each constituent; (iii) polarizability of ceramic particles and polymer; and (iv) nature of inter-connection between these particles [6–8].

P. Guggilla (✉) · A. K. Batra · M. E. Edwards
Department of Physics, Alabama A&M University,
P.O. Box 1268, Normal, AL 35762, USA
e-mail: padmaja.guggilla@aamu.edu

The simplest type of pyroelectric ceramics–polymer composite is 0–3 connectivity, a composite material comprising of pyroelectric ceramic powder particles embedded in polymer material.

Recently, composite polymer–ceramic have been prepared and characterized for piezoelectric and pyroelectric properties. Researchers have fabricated 0–3 connectivity composites using ferroelectric copolymer P(VDF–TrFE) as a host material. Electro-active ceramics used were lead lanthanum zirconate titanate (PLZT), lead titanate (PT), calcium-modified lead titanate (Ca-PT), lead magnesium niobate–lead titanate (PMN–PT), and others. With the apprehension in the environmental pollution of PbO evaporation, lead free ceramics have recently attracted substantial interest to replace the lead-based materials systems [9]. Lithium tantalite is a very attractive material due to its nonlinear optical properties, large electro optic, and pyroelectric coefficients [10]. $LiTaO_3$ has a high Curie temperature of 610 °C and a large spontaneous polarization. Polyvinylidene fluoride–trifluoroethylene [P(VDF–TrFE)] copolymer is a very commonly used ferroelectric polymer possessing good piezoelectric and pyroelectric properties [4, 11]. Copolymers show their advantages over homopolymers in the interfacial region by increasing the fracture toughness of a joint (point of contact of mers) [12]. This study focuses on the description of fabrication of 0–3 connectivity composite films of Lithium tantalate ($LiTaO_3$–99.9% designated as LT in this paper) nanoparticles dispersed in polyvinylidene fluoride–trifluoroethylene [P(VDF–TrFE) 70/30 mol%] using 'solvent cast' method. As the properties of the ceramics and polymers are tailored in composites, the weight percentage of ceramic is varied to suit specific applications. The dielectric and pyroelectric properties of the composite films with different wt% of LT are investigated with variation in frequency as well as temperature and compared with the pure P(VDF–TrFE) and pure $LiTaO_3$ single crystal.

Experimental

The 0–3 composite samples were prepared by 'solvent cast' method (SC). In this method, a measured quantity of polyvinylidene fluoride–trifluoroethylene 70/30 mol% copolymer obtained from Measurement Specialties Inc, PA was dissolved in methyl-ethyl-ketone (MEK) at room temperature. A known amount of lithium tantalite 99.9% (LT) powder procured from a Johnson Matthey Company, MA was added to the copolymer solution. Suspension was dispersed using an ultrasonic agitation bath and a magnetic stirrer for 15–30 min for uniform mixing of the particles into the matrix. The mixture was continuously stirred by varying the temperature from room temperature to 60 °C.

The solution was kept overnight for solvent to evaporate. The films so obtained were later kept at a temperature of 100–120 °C for annealing and to remove solvent. The same procedure was followed to obtain films of different wt% of LT. Typically, thickness of the films were 80–100 μm. The samples were cut and silver electroded for electrical measurements. As the LT and P(VDF–TrFE) have pyroelectric coefficients of similar sign sample, poling reinforces the pyroelectric activity of the sample. Depending upon the direction of the applied field, the copolymer phase can be poled in the same direction (parallel polling) or in opposite directions (anti-parallel) to the ceramic polarization [13]. The electroded samples were poled at 100 °C with an electric field of 5 MV/m for 2 h. After the poling process, the samples were short circuit annealed at 50 °C for 2 h. The wt% of LT powder in polymer matrix chosen for the present was 0.9% (sample named LT5), 0.7% (LT4), and 10% (LT2).

To measure the capacitance and dielectric loss, a QuadTech 1920 LCR Bridge interfaced to computer was used. The sample under test to measure the capacitance was placed at a close contact with the heating element inside a shielded sample holder. The complete setup includes a QuadTech® Model 1920 precision LCR meter, an Agilent 34970A DMM (Digital Multimeter) with a Type K Thermocouple input for temperature measurement, a Barnant Company Model 669 Temperature Control Unit with a Type K Thermocouple input for feedback loop control, a Staco, Inc. Type 3PN1010 Variac for heater power adjustment, and a PC. All the instruments were connected to the computer for data acquisition at specified time intervals through a GPIB plug and controlled by LabVIEW software. The capacitance (Cp) and dissipation factor (tan δ) at frequencies from 10 Hz to 1 MHz with an applied electric field of $\sim$1 V/cm were measured at different temperatures. The temperature is increased at a constant rate of 1 °C/min and the test fixture is allowed to reach isothermal conditions and then another set of measurements were taken. The reading was taken at 10 °C interval with a constant increment in temperature up to 10 °C.

Dielectric constant ε' (real part of the dielectric constant) is calculated from the following equation:

$$\varepsilon' = C_p \left(\frac{d}{A\varepsilon_0} \right) \tag{1}$$

where C_p is the parallel capacitance, ε_0 is the permittivity of free space which is 8.85×10^{-12} F/m, d is film thickness, and A is the electrode area, ε' is real part of the dielectric constant, and D (tan δ) is the dissipation factor [14–16].

Imaginary dielectric constant (ε'') is calculated by the equation

$$\varepsilon'' = \varepsilon'D \qquad \tan\delta = \frac{\varepsilon''}{\varepsilon'} \qquad (2)$$

where D is dissipation factor.

Capacitance of the samples obtained from the Quad-Tech® Model 1920 precision LCR (inductance, capacitance, resistance) meter at room temperature was used in finding the piezo voltage (G_{33}). D_{33} meter supplied by KCF Technologies Inc, PA was used in measuring piezoelectric coefficient (D_{33}) in pC/N by directly applying the stress in the thickness direction of the samples. At room temperature, the relative dielectric constant (ε_{33}) and piezo voltage (G_{33}) in Vm/N of all the samples were calculated from the following equations:

$$\varepsilon_{33} = \frac{T * C}{S * \varepsilon} \quad \text{and} \quad G_{33} = \frac{D_{33}}{\varepsilon_{33}} \qquad (3)$$

where T is thickness of the sample (m), S is area of the sample (m^2), C is capacitance of the sample (F), and $\varepsilon_0 = 8.85 \times 10^{-12}$ F/m.

To measure the dynamic pyroelectric current, direct method of Byer and Roundy [17] was used. The details of this method are given in author's earlier papers [6]. The pyroelectric current I_p was measured, and the pyroelectric coefficient (p) was calculated using a relationship [14–16].

$$p = \left(\frac{I_p}{A}\right) \bigg/ \left(\frac{dT}{dt}\right), \qquad (4)$$

where A is the electrode area (identical areas for the opposite electrodes used in each sample), and dT/dt is the rate of change of temperature which was kept constant. Figure 1 describes the experimental setup used for dielectric and pyroelectric current measurements.

To provide the measure of the efficiency of a given material for pyroelectric applications, the figures-of-merit are defined. By using the foregoing electrical parameters, the following material figure-of-merits for assessing the characteristics of single element pyroelectric detector, operating in optimum manner, were calculated as follows [18]:

$$F_I = p/c' \quad \text{for high current responsivity,} \qquad (5)$$

$$F_v = p/(c'\varepsilon') \quad \text{for high voltage responsivity, and} \qquad (6)$$

$$F_D = p/(c'\sqrt{\varepsilon''}) \quad \text{for high detectivity,} \qquad (7)$$

where p, c', ε', and ε'' are the pyroelectric coefficient, the volume specific heat, and the real and imaginary parts of the dielectric constant, respectively.

Results and discussion

Figure 2 shows the temperature dependence of the pyroelectric coefficient (p) of the 0–3 composite with various wt% of LT in polymer matrix. The figure depicts that all the poled samples were functional. It is found that pyroelectric coefficient increases with the increase of LT wt% in the polymer matrix. P(VDF–TrFE):LT2, the composite with the highest wt% among the three samples investigated, shows the highest pyroelectric coefficient at a given temperature. From the variation of pyroelectric coefficient with temperature with various wt% of LT in P(VDF–TrFE) polymer matrix, it was also evident that the pyroelectric coefficient of all the 0–3 composites are higher than pure P(VDF–TrFE).

The electrical response is very important as the permittivity is involved in the calculation of figures-of-merit. Dielectric constants (ε', ε'') of the composites measured at various temperatures and frequencies are presented in Figs. 3, 4, 5, 6, and 7. The dielectric constant depends on the applied frequency of signal as there would be a relaxation time for charge transport. At lower frequencies, the increment in the value of the ε' is very tiny and remained almost constant at higher frequencies. The large values of

Fig. 1 Block diagram of the experimental setup for pyroelectric and dielectric measurements
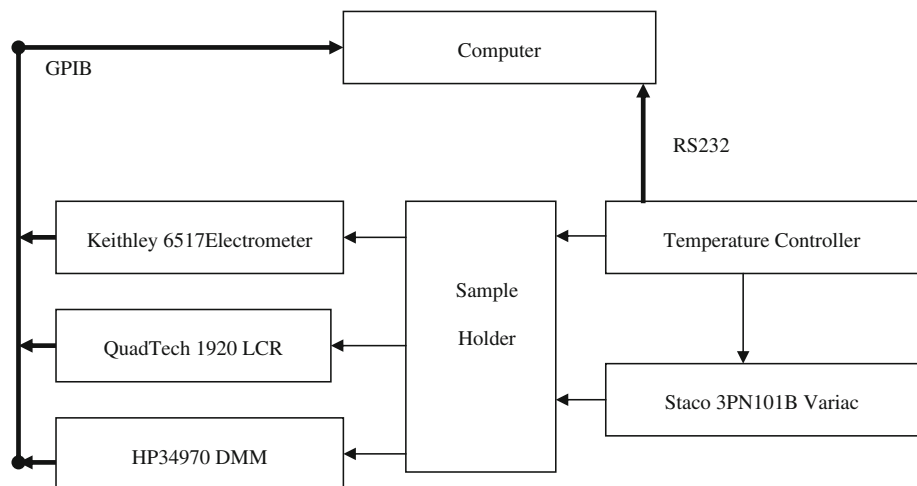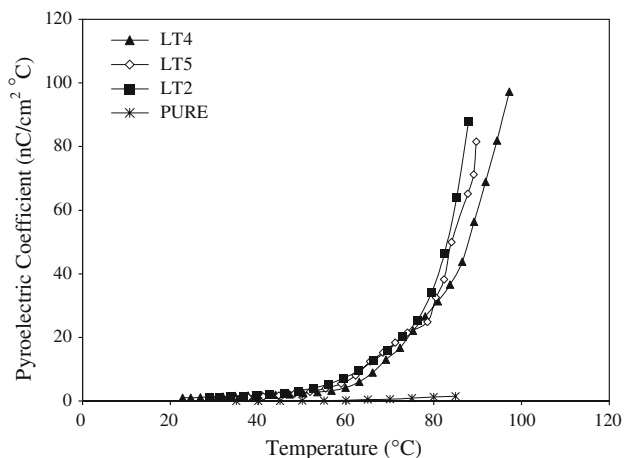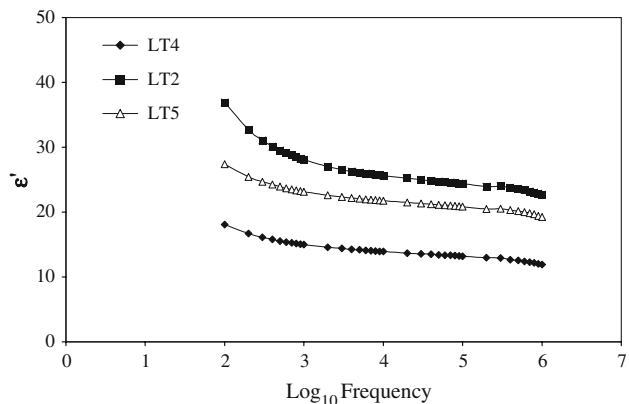
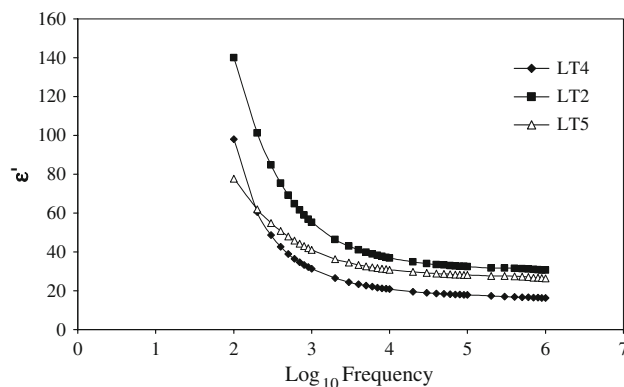**Fig. 2** Variation of pyroelectric coefficient with temperature for pure, LT2, LT4, and LT5 composites
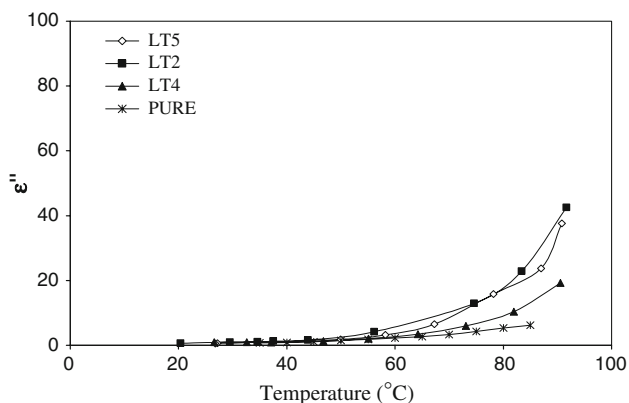
Fig. 3 Variation of imaginary part of dielectric constant (ε'') of LT2, LT4, and LT5 with temperature at 1000 Hz frequency
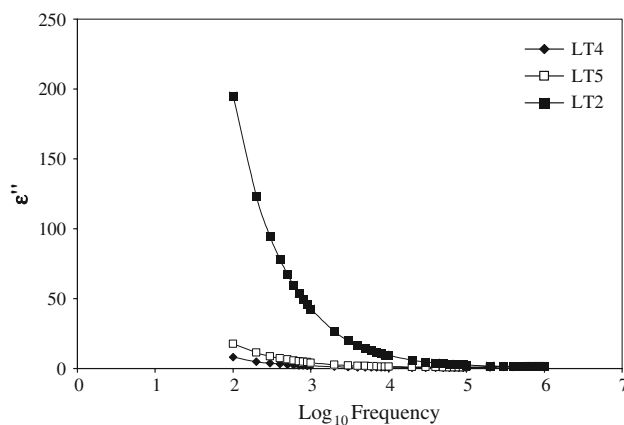

Fig. 4 Variation of real part of dielectric constant (ε') with frequency at 50 °C for LT2, LT4, and LT5

Fig. 5 Variation of real part of dielectric constant (ε') with frequency at 90 °C for LT2, LT4, and LT5

Fig. 6 Variation of imaginary part of dielectric constant (ε'') of LT2, LT4, and LT5 with frequency at 50 °C

Fig. 7 Variation of imaginary part of dielectric constant (ε'') of LT2, LT4, and LT5 with frequency at 90 °C
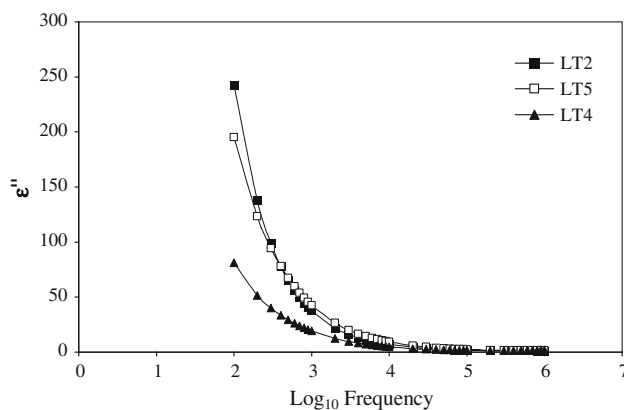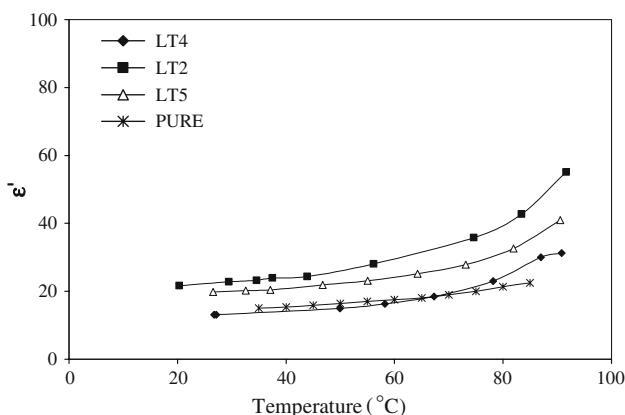
ε' was the resultant of the heterogeneity of the samples [19, 20]. The higher dielectric constant at low frequency may also be attributed to the effect of two-phase interface polarization [21]. The fall of dielectric constant ε' from low frequency to high frequency was attributed to the fact that ferroelectric regions are surrounded by similar relaxor ferroelectric materials [22]. At higher frequencies, only the electronic polarizability contributes to the polarization and therefore the dielectric constant remains unchanged [23]. In the figures shown, the dielectric constant (ε') falls rapidly

in the beginning for the composition having higher values of dielectric constant indicating that dispersion is high in composition with large value of ε'. There are more interfaces in high LT content sample, so ε' reduces faster than low LT content samples.

From Fig. 8, it is seen that ε' increases slowly with temperature which is the predicted phenomenon in pyroelectric materials. An increase in dielectric constants (ε', ε'') with wt% of LT powder in polymer matrix was found. Increase in the ε' value with increased LT wt% was due to higher permittivity of LT as compared to P(VDF–TrFE) copolymer. The increase of ε'' with LT content may be due to leakage conductive loss [6, 15]. The tan δ is proportional to the imaginary part of the dielectric constant ε'', is the energy dissipation in the dielectric system. Precisely, the variation of loss tangent (tan δ) with frequency for all the composites shows a similar dispersion as that of dielectric constant with frequency.

Table 1 lists the physical properties of important pyroelectric materials such as $LiTaO_3$ crystal and pure P(VDF–TrFE) along with this study. Using Eq. 3, values of piezoelectric coefficient (d_{33}) and piezo voltage (G_{33}) are calculated and they show an increase in the values with the increase in the LT weight percentage in the P(VDF–TrFE) polymer matrix.

Figures-of-merit determine the material's usefulness for use in IR detector applications. Using Eqs. 5–7 values of the figures-of-merit are calculated. The figure-of merits (F_I, F_D) of the pyroelectric composites investigated are lower than candidate single crystal $LiTaO_3$ but higher than pure P(VDF–TrFE) polymer. From the results obtained, the composites of LT:P(VDF–TrFE) are suitable where higher voltage responsivity is of main interest. However, considering the time and cost of growing single crystals, LT:P(VDF–TrFE) composite may still be useful for low level applications where large area, flexible with high strength, and low cost sensor elements are required. Furthermore, with composite materials film IR detector fabrication, there is no need of lapping and polishing as is required in single crystals processing. Furthermore, according to Dias and Das-Gupta, the composites, however, have the advantage of being easier to polarize in thicker self-supporting samples, thus preventing the need of a substrate for the fabrication of IR sensor. Other advantage being, detectors can also be integrated with silicon technology as has been demonstrated in the past [6, 12, 24].

Conclusions

The experimental result obtained of P(VDF–TrFE):LT 0–3 connectivity composite can be summarized as follows:

Fig. 8 Variation of real part of dielectric constant (ε') of pure, LT2, LT4, and LT5 with temperature at 1000 Hz frequency

Table 1 Physical properties and figure-of-merits of various pyroelectric materials

Parameter	Units	LiTaO₃ (crystal) (LT)	P(VDF–TrFE) [18]	P(VDF–TrFE):LT5 (this study) @ 65 °C	P(VDF–TrFE):LT4 (this study) @ 65 °C	P(VDF–TrFE):LT2 (this study) @ 65 °C
P	$\mu Cm^{-2}\ °C^{-1}$	180	26.4	80.6	71.5	89.8
ε'	–	47	9.20	23.1	25.6	28.1
tan δ	–	0.005	0.024	0.07	0.09	0.15
ε''	–		0.235	0.22	1.17	2.31	4.22
c'	10^6 J m^{-3} °C^{-1}	3.2	2.09	2.1	2.1	2.1
d_{33}	pC/N	8	4.3	3.0	5.0	7.0
G_{33}	Vm/N	0.17	0.467	0.129	0.195	0.249
F_V	10^{-6} μC J^{-1} m	1.19	0.16	1.66	1.33	1.52
F_I	10^{-6} μC J^{-1} m	56.25	12.6	38.38	34.05	42.76
F_D	10^{-6} μC J^{-1} m	116.05	8.96	35.48	22.4	20.82

P(VDF–TrFE):LT5 composite: 0.9 wt% of lithium tantalate particles in P(VDF–TrFE) matrix

P(VDF–TrFE):LT4 composite: 0.7 wt% of lithium tantalate particles in P(VDF–TrFE) matrix

P(VDF–TrFE):LT2 composite: 10 wt% of lithium tantalate particles in P(VDF–TrFE) matrix

(i) Films of LT:P(VDF–TrFE) composites with various amount of lithium niobate (LT) powder/particles have been fabricated using 'solution cast' method. This technique is very attractive for manufacturing pyroelectric sensor because of the low processing temperatures and less time than growing LT single crystals.

(ii) The composites were characterized for their dielectric and pyroelectric properties, in order to determine their usefulness in uncooled IR detector applications.

(iii) The dielectric constants (ε', ε'') and pyroelectric coefficient (p) of the composite were found to increase with the increase in the amount of LT particles dispersed in P(VDF–TrFE) polymer matrix.

(iv) Higher the content of the LT is beneficial for the piezoelectric performance of the 0–3 type LT:P (VDF–TrFE) composites.

(v) Obtained values of D_{33} and G_{33} are close to the literature values which manifests that the LT particles were uniformly dispersed in the P(VDF–TrFE) polymer matrix.

(vi) The calculated pyroelectric figures-of-merits (F_I, F_V, F_D) of the composites were found to be higher than pure P(VDF–TrFE).

(vii) Based on the results obtained, LT:P(VDF–TrFE) films are a good lead free candidates as IR sensing elements, especially where curved surface detectors are needed due to its flexibility and high strength of films.

References

1. Dorey RA, Whatmore RW (2005) J Eur Ceram Soc 25:2379
2. Van Valck LH (1989) Elements of materials science and engineering, 6th edn. Prentice Hall, pp 347–372
3. Corker DL, Zhang Q, Whatmore RW, Perrin C (2002) J Eur Ceram Soc 22:383
4. Koga K, Ohigashi H (1986) J Appl Phys 56(6):2142
5. NG KL, Helen LWC, Choy CL (2000) IEEE Trans Ultrason Ferroelectr Freq Control 47:1308
6. Aggarwal MD, Currie JR, Penn BG, Batra AK, Lal RB (2007) NASA/TM-2007-215190
7. Newnham RE, Skinner DP, Cross LE (1978) Mat Res Bull 13:525
8. Tressler JF, Alkoy S, Newnham RE (1999) Composites A 30:477
9. Kwok-ho L, Xiaoxing W, Helen L (2005) Composites A 36:1595
10. Weis RS, Gaylord TK (1985) Appl Phys A 37:191
11. Furukawa T, Johnson GE, Bair HE (1981) Ferroelectrics 32:61
12. Carl AK (1985) Materials science in engineering, 4th edn. Elsevier Science Series
13. Lam KH, Chan HLW (2005) Compos Sci Technol 65:1107
14. Dias CJ, Das-Gupta DK (1996) IEEE Trans Die Elect Ins 3(5):706 and references therein
15. Batra AK, Simmons M, Guggilla P, Aggarwal MD, Lal RB (2004) Integr Ferroelectr 63:161
16. Lang SB, Das-Gupta DK (2000) Ferroelectr Rev 2:217
17. Byer RL, Roundy CB (1972) Ferroelectrics 3:333
18. Lal RB, Batra AK (1993) Ferroelectrics 142:51
19. Kothale MB, Patankar KK, Kadam SL, Mathe VL, Rao AV, Chougule BK (2002) Mater Chem Phys 77:691
20. Vishvanathan B, Murthy VRK (1990) Ferrite materials science and technology. Narosa Publishing House, New Delhi, p 219
21. Zhai JY, Cai N, Liu L, Lin YH, Nan CW (2004) J Phys D Appl Phys 37:823
22. Upadhyay S, Kumar D, Prakash O (1996) Bull Mater Sci 19:513
23. Keer HV (1993) Principles of the solid state, 1st edn. New Age International Publishers, pp 302–330
24. Kulkarni SR, Kanamadi CM, Chougule BK (2005) Mater Res Bull 40:2064